Electronic Supplementary Material (ESI) for Chemical Communications.

Halogen Ion-Selective Phosphorescence Turn-on Probe Based on Induction of Pt-Pt Interactions

Jing Yang,[a] Lili Sun,[b] Liang Hao,[a] Gang-Gang Yang,[a] Zhi-Cong Zou,[a] Qian Cao,*[a] Liang-Nian Ji,[a] and Zong-Wan Mao*[a]

[a] MOE Key Laboratory of Bioinorganic and Synthetic Chemistry, School of Chemistry, Sun Yat-Sen University, Guangzhou 510275, China
[b] School of Materials Science and Engineering, Sun Yat-Sen University, Guangzhou 510275, China
E-mail address: caoqian3@mail.sysu.edu.cn (Q. Cao); cesmzw@mail.sysu.edu.cn (Z.-W. Mao)

MATERIALS AND METHODS

K_2PtCl_4 (Alfa Aesar), 2,2-bipyridine (J&K Scientific Ltd.), Imidazole, $Ag(CF_3O_3S)$, AgNO3, AgCl (Sigma Aldrich), cisplatin, DMSO (dimethyl sulfoxide, Sigma Aldrich), MTT (3-(4,5-dimethylthiazol-2-yl)-2,5-diphenyltetrazolium bromide, Sigma Aldrich), $Ru(bpy)_3Cl_2$ (J&K Scientific Ltd.); ABDA(9,10-Anthracenediyl-Bis(methylene), Sigma Aldrich) . NH_4PF_6 was purchased from Alfa Aesar; MTDR (MitoTracker Deep Red) & LTDR (LysoTracker Deep Red) was purchased from Life Technologies, USA;

All of the compounds tested were dissolved in DMSO immediately prior to the experiments, and the final concentration of DMSO was kept at 1% (v/v). NMR spectra were recorded on a Bruker Avance 400 spectrometer. Shifts were referenced relative to the internal solvent signals. Microanalysis (C, H, and N) was carried out using an Elemental Vario EL CHNS analyser (Germany). UV–vis spectra were recorded on a Varian Cary 300 spectrophotometer (USA). Emission spectra were recorded on a Shimadzu RF-5301 PC spectrofluorophotometer. ESI-MS spectra were recorded on a Thermo Finnigan LCQ DECA XP spectrometer (USA). The quoted m/z values represent the major peaks in the isotopic distribution. Conforcal images were captured by Conforcal Telescope (Germany, Carl Zeiss LSM 710), Lifetime was recorded by a DPC-23016 Channel Photon correlator (Becker &Hickl GmbH, UK).

Characterizations of Cyclometalated Pt(II) complexes

The chloro-bridged dimer, $[Pt(ppy)_2Cl]_2$ were synthesized following literature methods[1]. For synthesis of **Pt1**-OTF, NO_3, Pt dimer was dechloried in DMF by corresponding silver salt anions ($CF_3O_3S^-$, NO_3^-) at 298 K for 24 h, for synthesis of **Pt1**-Cl, dechloried in DMF by silver salt was not required as reported [2]. The AgCl precipitate was filtered off and indicated equiv of 2,2-bipyridine (bpy), 1,10-Phenanthroline hydrate (phen)(1-fold eqv) or Imidazole (Imazo)(5-fold eqv) was added into the filtrate respectively. After stirred for 24 hours, the precipitate was filtered and washed by ether. All the complexes were purified by recrystallization and characterized by ESI-MS, ^1H NMR spectroscopy, and elemental analysis.

Pt1-OTF: A mixture of precursor $[Pt(ppy)Cl]_2$ (0.09 mmol, 0.100 mg) and $AgCF_3SO_3$ (0.18 mmol, 47.5 mg) in CH_3CN (30 mL) was refluxed overnight. After removing off-white AgCl precipitate, the remaining solution was evaporated to obtain yellow solids $[Pt(ppy)(CH_3CN)_2]^+$, 1,4-bipyridine (0.18 mmol, 28.9 mg) was added into 5 mL DMF solution of $[Pt(ppy)(CH_3CN)_2]^+$ and refluxed for 24 h under N_2 protection. Then 30 mL diethyl etherther was added and precipitates were obtained, followed by diethyl ether and water wash. The final product was red brown powder, yield: 0.640 g (70%). ESI-MS (CH_3OH): m/z 505.68, $[M\text{-}OTF]^+$. Elemental analysis: calcd (%) for $C_{22}H_{18}N_3O_4F_3SPt \cdot 2H_2O$: C, 38.26; H, 2.92; N, 6.08; found: C, 38.24; H, 2.93; N, 6.09; 1H NMR (400 MHz, DMSO-d6, 4.5mM) δ 9.28 (d, J = 5.3 Hz, 1H), 9.00 (d, J = 4.9 Hz, 1H), 8.83 (d, J = 5.7 Hz, 1H), 8.63 (dd, J = 17.0, 8.0 Hz, 2H), 8.49 – 8.35 (m, 2H), 8.23 – 8.06 (m, 2H), 7.95 – 7.86 (m, 1H), 7.83 – 7.69 (m, 2H), 7.42 (t, J = 6.3 Hz, 1H), 7.31 – 7.11 (m, 3H)

Pt1-NO_3: The synthesis is similar to that of **Pt1-OTF**, except that the dechlorination of $[Pt(ppy)Cl]_2$ (0.09 mmol, 0.100 mg) was operated in DMF by adding $AgNO_3$ (0.18 mmol, 31.42 mg) instead of $AgCF_3SO_3$. The final product was light-red powder, yield: 0.320 g (40%). ESI-MS (CH_3OH): m/z 505.45, $[M-NO_3]^+$. Elemental analysis: calcd (%) for $C_{21}H_{16}N_4O_3Pt \cdot H_2O$: C, 43.08; H, 3.10; N, 9.57; found: C,43.09, H, 3.08; N, 9.56; ^{1}H NMR (400 MHz, DMSO-d6) δ 9.15 (d, J = 5.1 Hz, 1H), 8.87 (d, J = 4.7 Hz, 1H), 8.69 (d, J = 5.3 Hz, 1H), 8.49 (dd, J = 17.1, 7.9 Hz, 2H), 8.36 – 8.26 (m, 2H), 8.06 (d, J = 7.4 Hz, 1H), 8.00 – 7.91 (m, 3H), 7.81 – 7.73 (m, 1H), 7.67 – 7.62 (m, 1H), 7.29 (t, J = 6.1 Hz, 1H), 7.12 – 7.05 (m, 2H).

Pt1-Cl: The synthesis is similar to that of **Pt1-OTF**, except that the dechlorination of $[Pt(ppy)Cl]_2$ was not required. Precursor $[Pt(ppy)Cl]_2$ (0.09 mmol, 0.100 mg) was solved in 5 mL DMF, then bpy (0.18 mmol, 28.9 mg) was added and refluxed for 24 h under N_2 protection. Then 30 mL diethyl etherther was added and precipitates were obtained, followed by diethyl ether and water wash. Finally, light red crystals of **Pt1-**Cl for X-ray analysis were obtained by slow diffusion of diethyl ether into DMSO solution of **Pt1-**Cl. Light-red powder, yield: 0.320 g (40%). ESI-MS (CH_3OH): m/z 505.33 $[M-Cl]^+$. Elemental analysis: calcd (%) for $C_{21}H_{16}ClN_3Pt$: C, 46.63; H, 2.98; N, 7.77; found: C,46.62, H,2.97; N, 7.74; ^{1}H NMR (400 MHz, DMSO-d6) δ 9.49 (d, J = 5.7 Hz, 1H), 8.69 (d, J = 4.1 Hz, 2H), 8.39 (d,

J = 8.0 Hz, 2H), 8.24 – 8.10 (m, 3H), 7.95 (td, J = 7.8, 1.7 Hz, 2H), 7.79 (dd, J = 7.4, 1.4 Hz, 1H), 7.55 – 7.43 (m, 3H), 7.17 (dq, J = 7.3, 5.9 Hz, 2H).

Pt2-OTF: The synthesis is similar to **Pt1-OTF**, except 5-folds of Imidazole (0.45 mmol, 31.48 mg) was used to react with Pt(ppy)($CH_3CN)_2$ instead of bpy. Finally, light yellow-green crystals of **Pt2-OTF** were obtained by slow diffusion of diethyl ether into the acetonitrile solution of **Pt2-OTF**. Light Green powder, yield:(50%). ESI-MS (CH_3OH): m/z 485.02, $[M-CF_3SO_3^-]^+$. Elemental analysis: calcd (%) for $C_{18}H_{16}F_3N_5O_3PtS\cdot 2H_2O$: C, 32.24; H, 3.01; N, 10.44; found: C, 32.24; H, 3.03; N, 10.42; ^{1}H NMR (400 MHz, DMSO-d6) δ 8.40 (s, 2H), 8.11 (d, J = 6.1 Hz, 3H), 7.80 (d, J = 5.7 Hz, 1H), 7.75 (d, J = 7.5 Hz, 1H), 7.50 (s, 1H), 7.44 (s, 1H), 7.31 (d, J = 16.1 Hz, 4H), 7.11 (t, J = 7.2 Hz, 1H), 7.02 (t, J = 7.2 Hz, 1H), 6.35 (d, J = 7.4 Hz, 1H).

Pt1a [Pt(ppy)(phen)]OTF: The synthesis is similar with **Pt1**-OTF, except 4-folds of 1,10-Phenanthroline (0.36 mmol, 66.68 mg) monohydrate was used to react with Pt(ppy)($CH_3CN)_2$ instead of bpy. Light Red powder, yield: (80%). ESI-MS (CH_3OH): m/z 529.52 $[M-CF_3SO_3^-]^+$.Elemental analysis: calcd (%) for $C_{24}H_{16}F_3N_3O_3PtS$: C,42.48; H, 2.38; N, 6.19 ; found: 42.50, H, 2.39; N, 6.17; ^{1}H NMR (400 MHz, DMSO-d6) δ 9.68 (d, *J* = 4.9 Hz, 1H), 9.42 (d, *J* = 3.8 Hz, 1H), 9.00 (d, *J* = 7.3 Hz, 2H), 8.93 (d, *J* = 5.6 Hz, 1H), 8.31 (d, *J* = 4.8 Hz, 2H), 8.21 (s, 1H), 8.08 (t, *J* = 7.4 Hz, 2H), 7.96 (d, *J* = 7.7 Hz, 1H), 7.59 (d, *J* = 7.3 Hz, 1H), 7.38 (d, *J* = 7.3 Hz, 2H), 7.16 (dt, *J* = 23.7, 7.2 Hz, 2H).

Crystallographic structure determination

Light red crystals of **Pt1-**Cl qualified for X-ray analysis were obtained by slowly precipitated from DMSO solution of **Pt1-**Cl, light yellow-green crystals of **Pt2** were obtained by slowly precipitated from CH_2Cl_2 solution of **Pt2**. Crystal structure of **Pt1-**Cl was collected by using CrysAlisPro (Rigaku OD, 2017) diffractometer (Cu-*K*, λ = 1.54184 Å) at 100(2) K. Multi-scan absorption correction was carried out with program CrysAlisPro. Single Crystal X-ray diffraction measurement of **Pt2**-OTF was performed on a Burker D8 QUEST diffractometer (Mo-K□, λ = 0.71073 Å) at 120(2) K. The data indexing and integration were performed by Bruker APEX3 program. Both crystal structures were solved by direct methods with program SHELXTL (2014/7) and Olex2, and all non-hydrogen atoms were refined using the full-matrix least-squares program SHELXL (2014/7)[3] with anisotropic displacement parameters. The hydrogen atoms were constrained to

idealized geometries suing a riding model. There are totally 383 Å voids in the lattice of **Pt1-**Cl, wherein the chloride anions and/or solvents should be accommodated disorderly. To satisfy charge neutrality for **Pt1-**Cl, we try to identify all Q peaks with intensity above 1.0 in the void to chloride atoms, and adjust their occupancies according the ellipsoid sizes and restrict the sum of occupancies being identical with the chemical conclusions. The refinement results manifest that all disordered chloride atoms show normal Ueq with SIMU restrictions. There is crystallographically-imposed symmetry in **Pt1**-Cl structure with the Pt atom at a site with 222-symmetry and concomitant disorder of the N and C-atom sites in the 2-phenylpyridine and 2,2-bipyridine ligands, thus, C/N sites coordinated to Pt are refined as 0.75 N and 0.25 C, according to the chemical conclusions. Besides, it should be noted that the C/N sites coordinated to Pt in **Pt2** complex are also concomitant disorder in the 2-phenylpyridine, we refine and allow them as 0.5 N and 0.5 C on the same site.

The Crystallographic Data Centre reference deposit numbers CCDC 1894809 and 1894804 for **Pt1-**Cl and **Pt2**-OTF contain the supplementary crystallographic information.

Calculation of quantum yields

Quantum yields of luminescence at room temperature were calculated according to literature procedures[4]. Solutions of $[Ru(bpy)_3](PF_6)_2$ were used as the standard, PBS (Φ_{em} = 0.042)[5]; All emission decays were obtained on freshly prepared samples.

Cell lines and culture conditions

MCF-7 cells were obtained from Experimental Animal Center of Sun Yat-sen University (Guangzhou, China). Cell was maintained in DMEM (Dulbecco's modified Eagle's medium, Gibco BRL). The cell was cultured in a humidified incubator, which provided an atmosphere of 5% CO_2 and 95% air at 37 °C. In each experiment, cells treated with vehicle control (1% DMSO) were used as the reference group.

Cell viability

Cells cultured in 96-well plates were grown to confluence. The compounds were dissolved in DMSO (1%, v/v), and diluted with fresh media immediately. The cells were incubated with two

concentrations of the tested compounds for 44 h at 37 °C. 20 μL of MTT solution was then added to each well, and the plates were incubated for an additional 4 h. The media was removed, and DMSO was added (150 μL per well) and incubated for 10 min with shaking. The absorbance at 595 nm was measured using a microplate reader (Infinite M200 Pro, Tecan, Männedorf, Switzerland).

Confocal imaging of cellular Cl^- anion by Pt1

MCF-7 cells were cultured in normal DMEM media to confluence, for Cl^- deficient ($c(Cl^-)$ = 4 mM and 0.5 mM) culture media environment, Tyrode's solution buffer was used to maintain osmotic pressure, the concentration of Cl^- ions can be ensured during solution preparation, the cell were cultured with each media for 5 h, then treated with complexes **Pt1** (50 μM) at 37 °C for 1 h. Cells were visualized by confocal microscopy immediately; λex=405 nm and λem=480± 20 nm for green channel, λem= 665 ± 20 nm for red channel.

Theoretical Calculation and Mechanism

The geometrical structure and the frontier molecular orbitals of pt(bpy)(ppy)cl were calculated using density functional theory (DFT)[6-7] by the GAUSSIAN 09 software package program[8]). The calculations were carried out by M06 as implemented in the D0.1 version of Gaussian 09 software package [9]. The basis set for Pt and I is SDD[10] and the basis set for other atoms is 6-311+G*. All the optimum structures were confirmed by the hessians. The second derivatives provided harmonic vibrational frequencies to verify the nature of the stationary points, which were not additionally corrected in this paper. The excited state is performed by Time-dependent density functional theory (TD-DFT) calculations[11].

Statistical analysis

All biological experiments were performed at least twice with triplicates in each experiment. Representative results were depicted in this report and data were presented as means ± standard deviations.

Supporting Figures and Tables

(1)

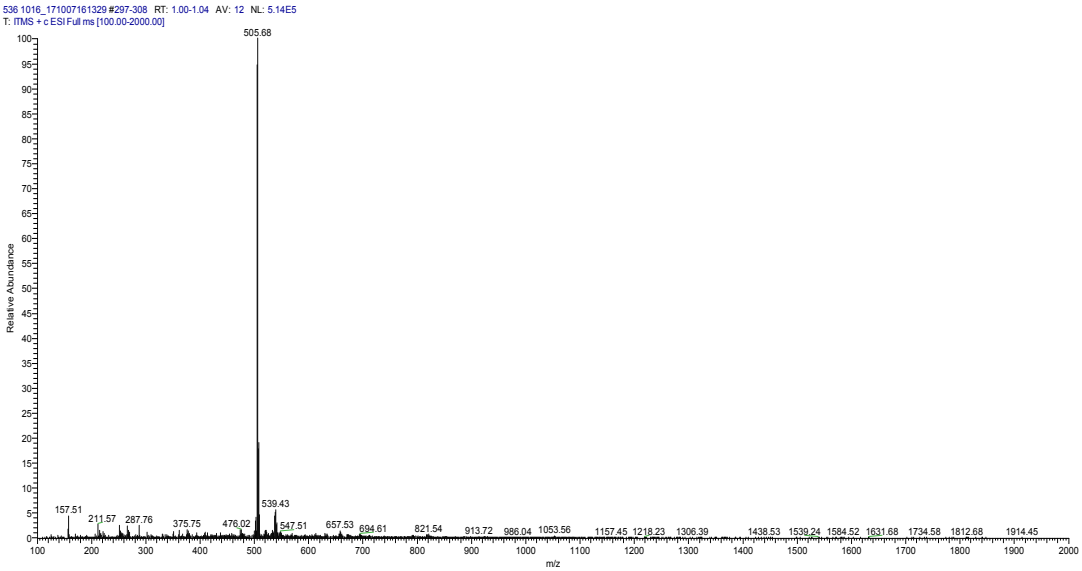

(2)

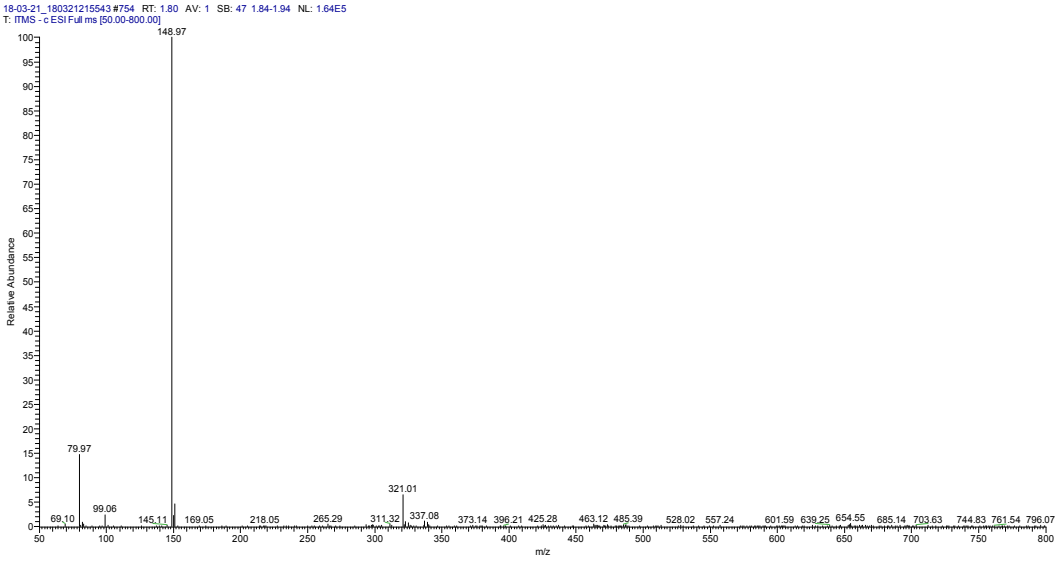

(3)

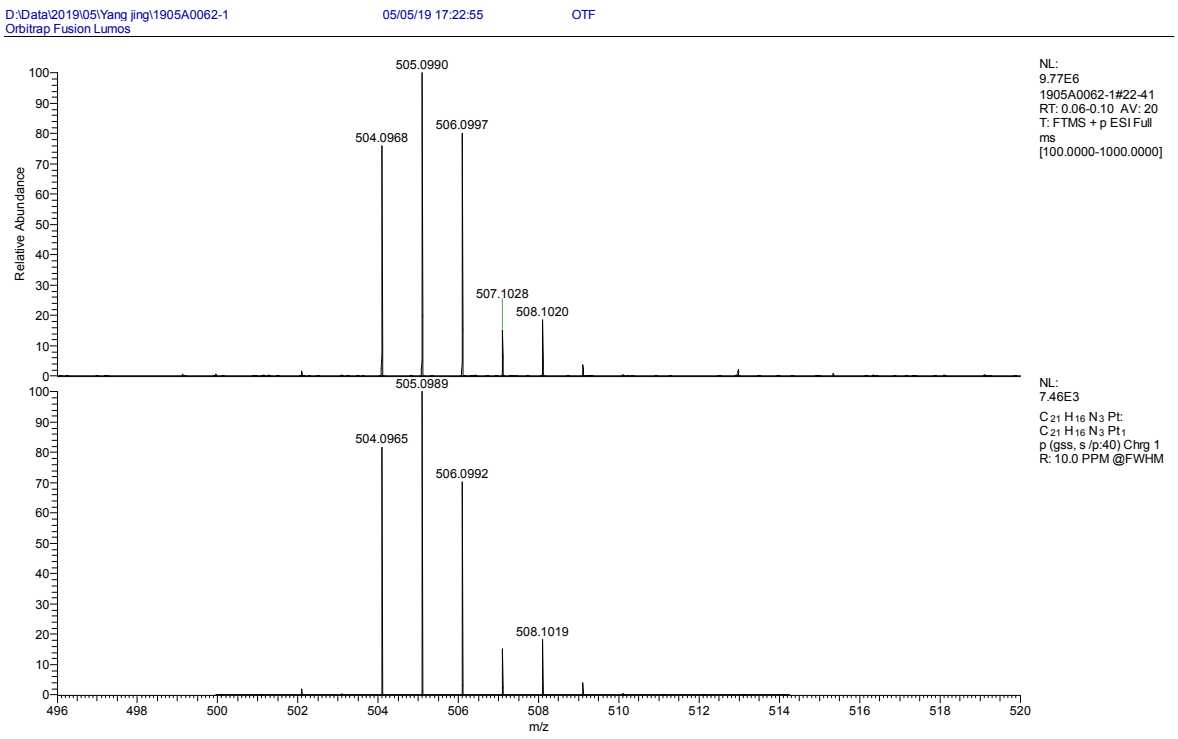

SPECTRUM - simulation :

m/z	Theo. Mass	Delta (ppm)	RDB equiv.	Composition
505.09901	505.09865	0.72	15.5	$C_{21}H_{16}N_3Pt$

(4)

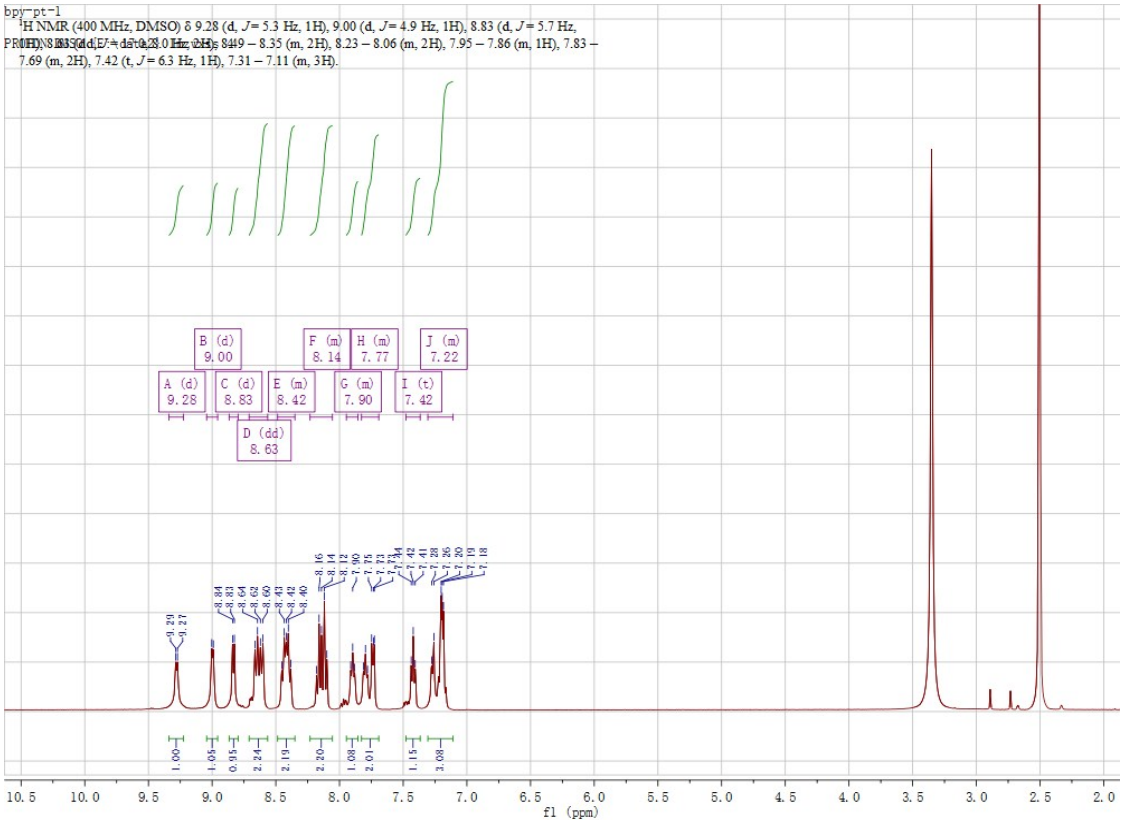

Fig. S1 (1) Positive and (2) Negative ESI-MS spectrum of **Pt1**-OTF; 505.65, $[M\text{-}CF_3SO_3^-]^+$; 148.97, $[CF_3SO_3]^-$; (3) High-resolution positive ESI-MS spectrum of **Pt1**-OTF, the data of mass peaks can be only assigned to a simulated fixed-composition of $[M\text{-}OTF]^+$;(4) ^{1}H NMR spectrum of complex **Pt1**-OTF (d_6-DMSO)

(1)

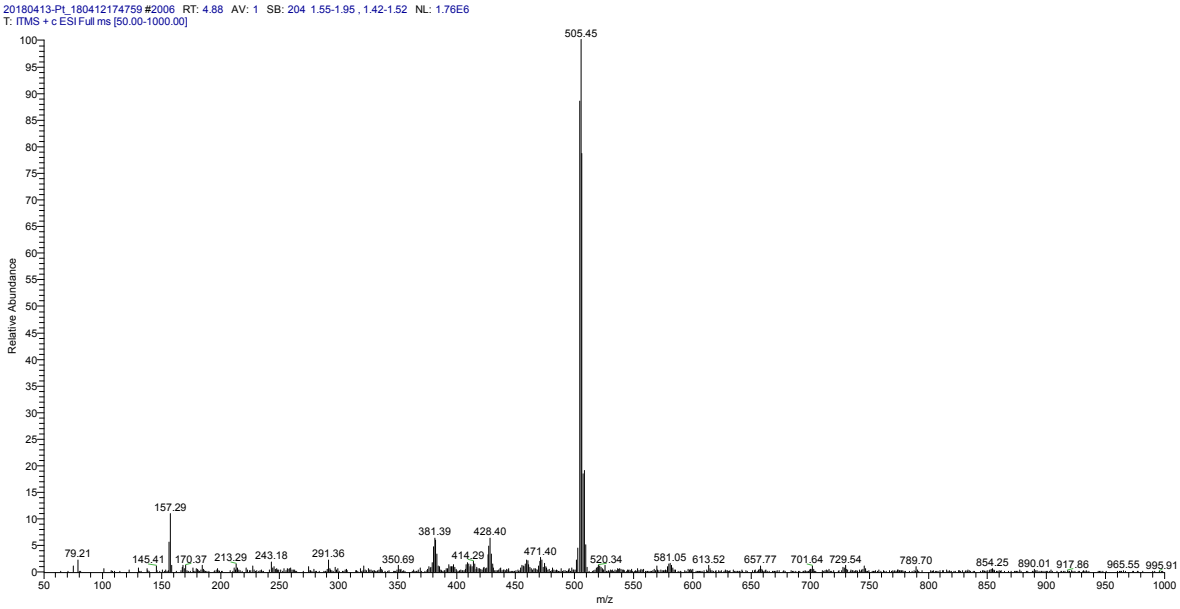
20180413-Pt_180412174759 #2006 RT: 4.88 AV: 1 SB: 204 1.55-1.95 , 1.42-1.52 NL: 1.76E6
T: ITMS + c ESI Full ms [50.00-1000.00]
Relative Abundance
m/z
505.45
157.29
381.39
428.40
79.21
145.41
170.37
213.29
243.18
291.36
350.69
414.29
471.40
520.34
581.05
613.52
657.77
701.64
729.54
789.70
854.25
890.01
917.86
965.55
995.91

(2)

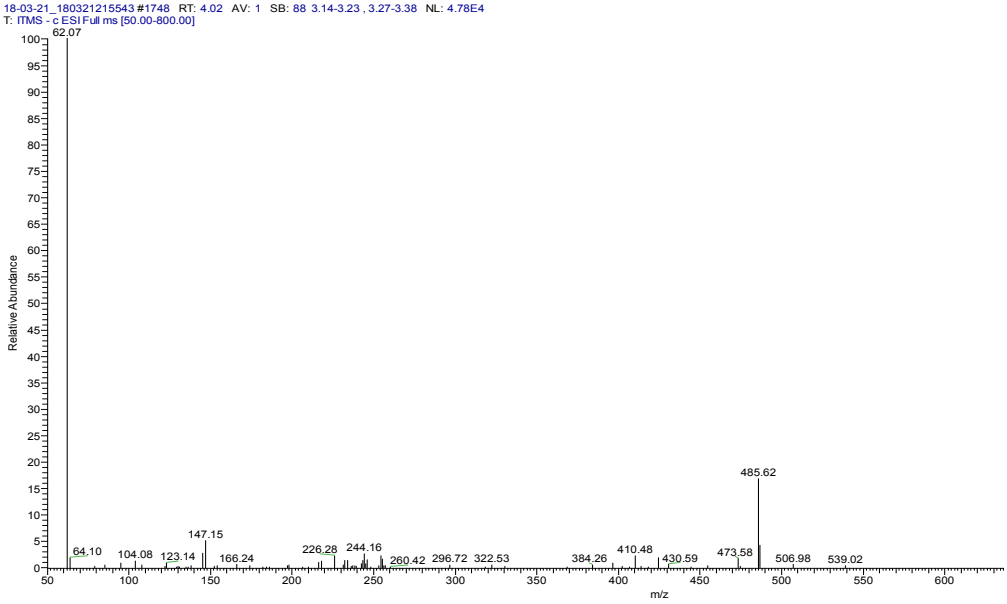
18-03-21_180321215543 #1748 RT: 4.02 AV: 1 SB: 88 3.14-3.23 , 3.27-3.38 NL: 4.78E4
T: ITMS - c ESI Full ms [50.00-800.00]
Relative Abundance
m/z
62.07
485.62
147.15
64.10
104.08
123.14
166.24
226.28
244.16
260.42
296.72
322.53
384.26
410.48
430.59
473.58
506.98
539.02

(3)

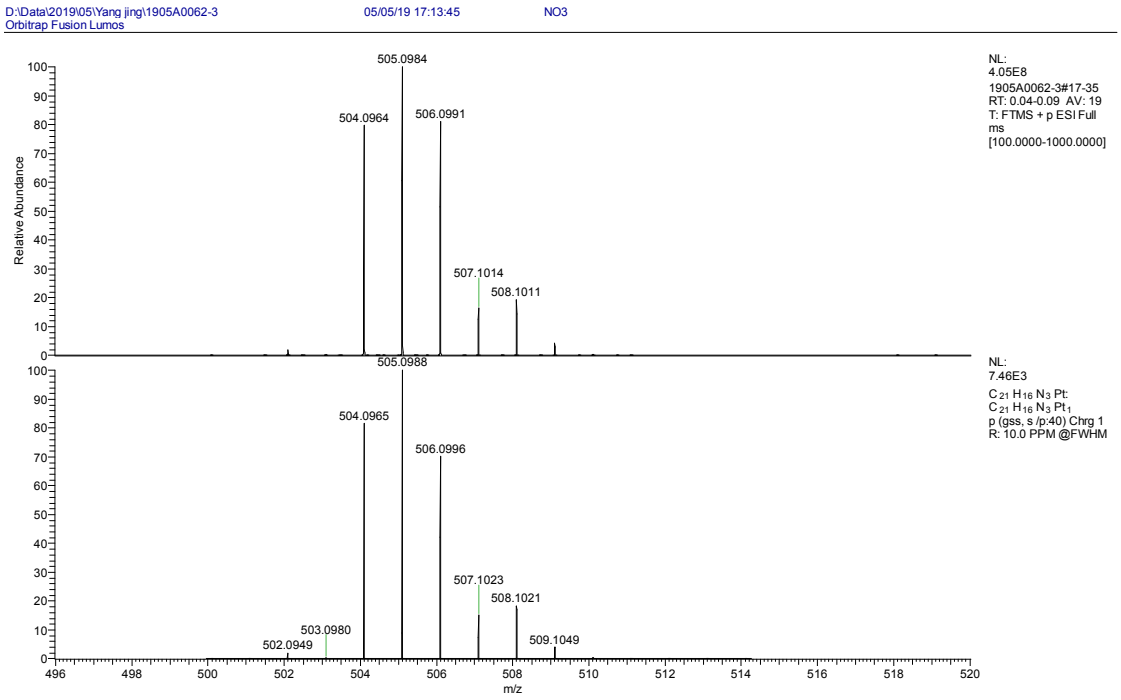

SPECTRUM - simulation :

m/z	Theo. Mass	Delta (ppm)	RDB equiv.	Composition
505.09847	505.09865	-0.35	15.5	C21 H16 N3 Pt

(4)

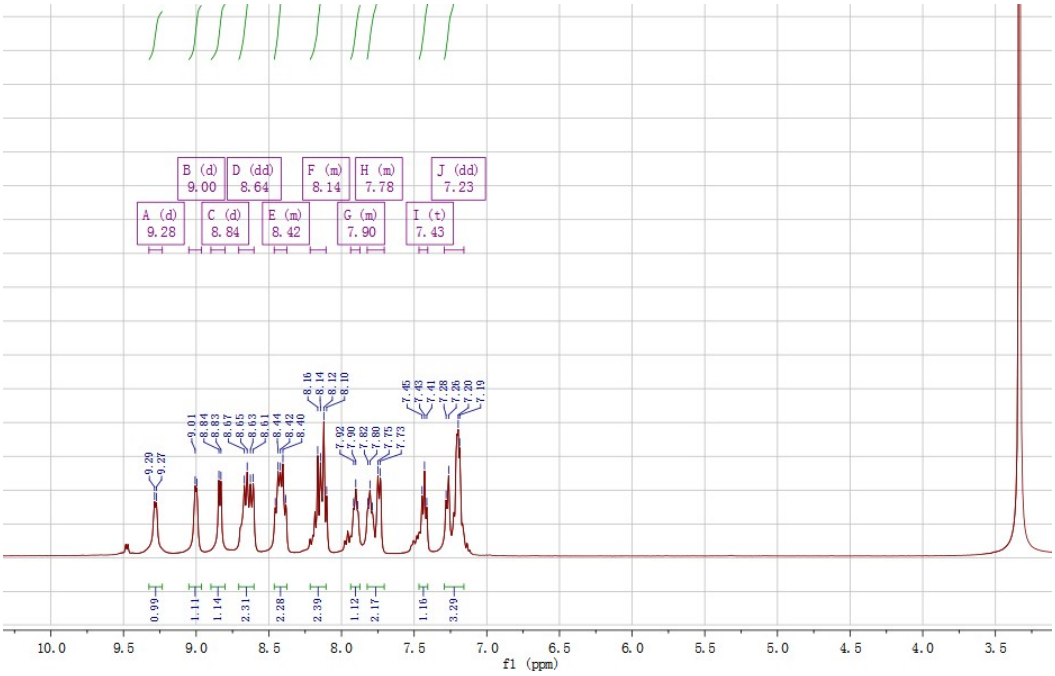

Fig. S2 (1) Positive and (2) Negative ESI-MS spectrum of **Pt1**-NO_3; 505.45, $[M\text{-}NO_3^-]^+$; 62.07, $[NO_3]^-$; (3) High-resolution positive ESI-MS spectrum of **Pt1-**NO_3, the data of mass peak can be only assigned to a simulated fixed -composition of $[M\text{-}NO_3]^+$;(4) ^{1}H NMR spectrum of complex **Pt1**-NO_3 (d_6-DMSO)

(1)

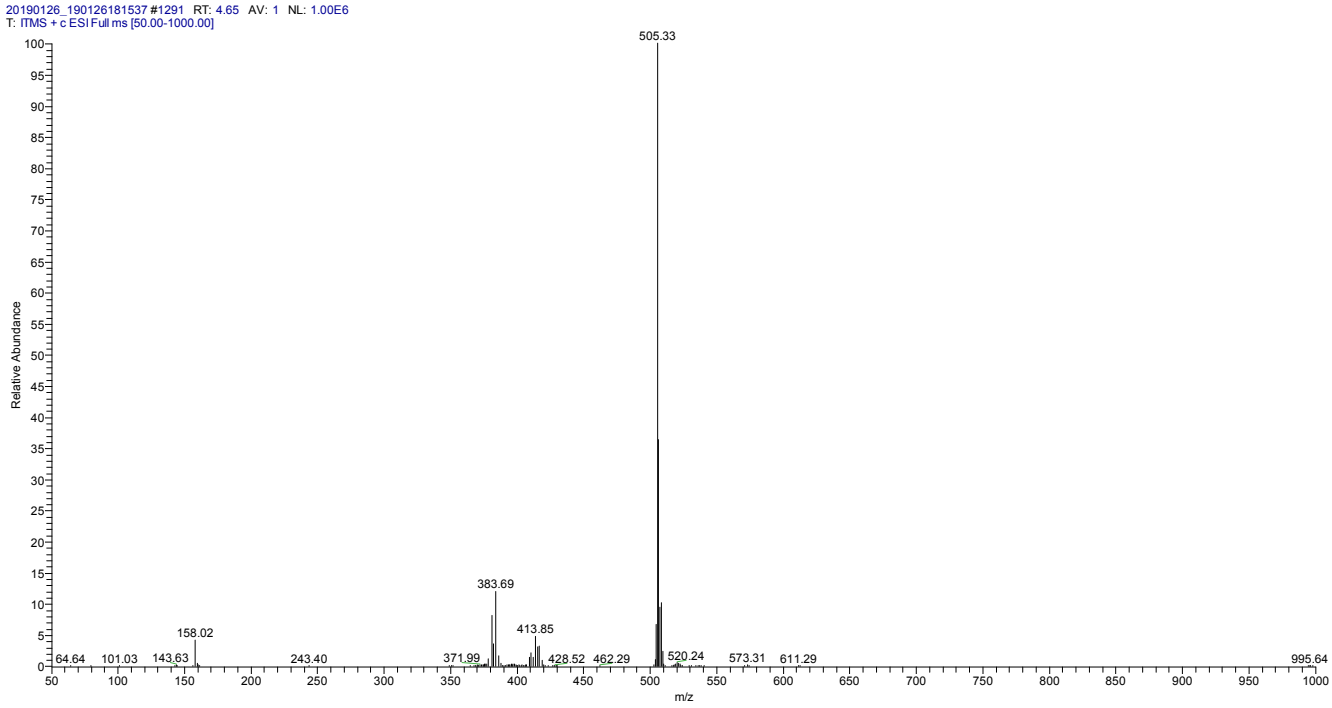
20190126_190126181537 #1291 RT: 4.65 AV: 1 NL: 1.00E6
T: ITMS + c ESI Full ms [50.00-1000.00]
Relative Abundance
m/z
505.33
383.69
158.02
413.85
64.64
101.03
143.63
243.40
371.99
428.52
462.29
520.24
573.31
611.29
995.64

(2)

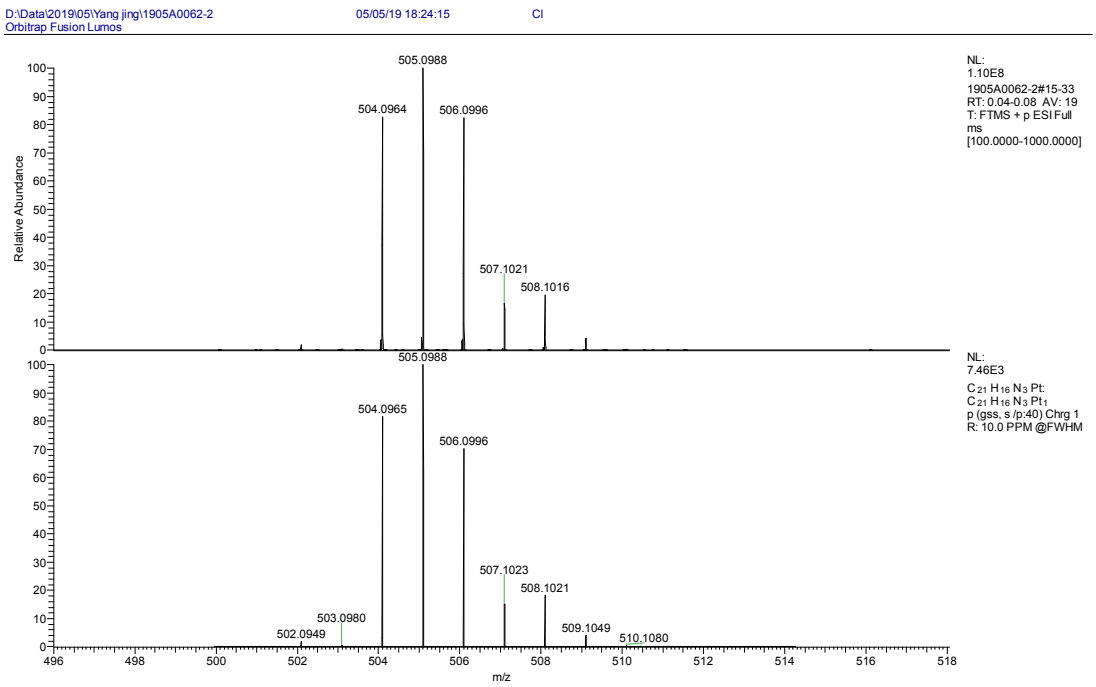

SPECTRUM - simulation :

m/z	Theo. Mass	Delta (ppm)	RDB equiv.	Composition
505.09877	505.09865	0.24	15.5	C21 H16 N3 Pt

(3)

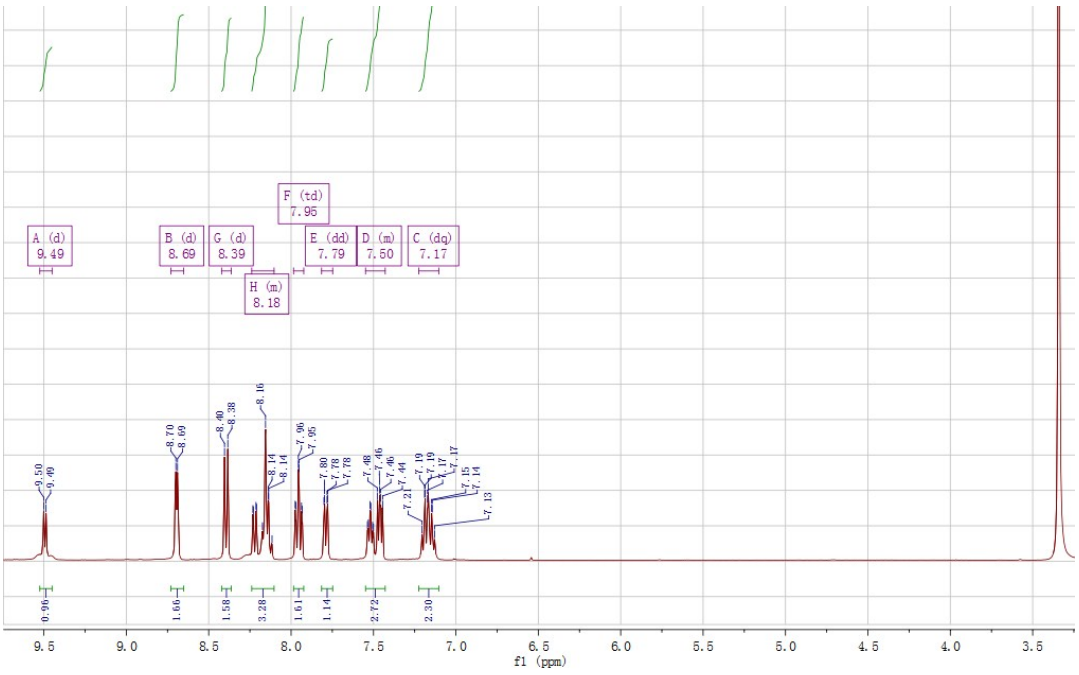

Fig. S3 (1) Positive ESI-MS spectrum of **Pt1**-Cl; 505.33, $[M\text{-}Cl^-]^+$; Negative ESI-MS spectrum of **Pt 1-**Cl: $[Cl^-]$ can not be detected. (2) High-resolution positive ESI-MS spectrum of **Pt1-**Cl, the data of mass peak can be only assigned to simulated fixed-composition of $[M\text{-}Cl]^+$; (3) ^1H NMR spectrum of complex **Pt1**-Cl (d_6-DMSO).

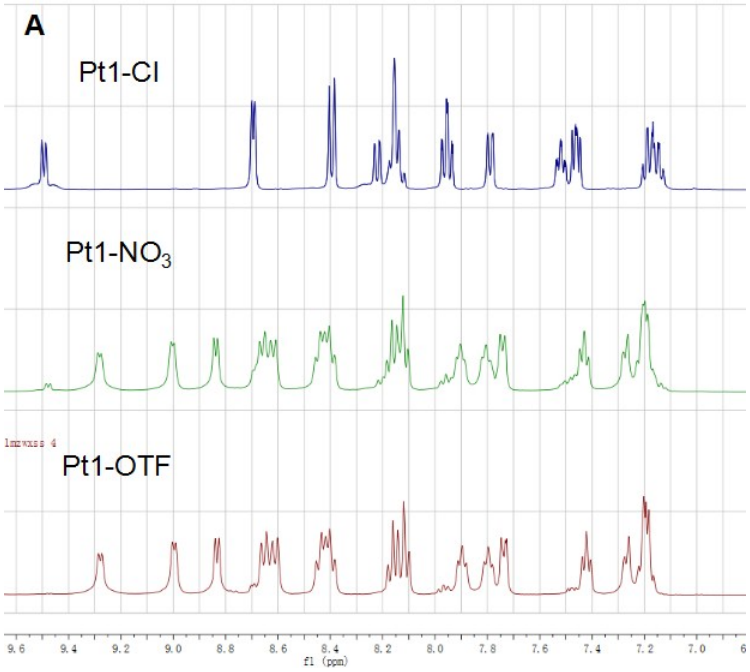
A
Pt1-Cl
Pt1-NO3
Pt1-OTF
9.6 9.4 9.2 9.0 8.8 8.6 8.4 8.2 8.0 7.8 7.6 7.4 7.2 7.0 6
f1 (ppm)

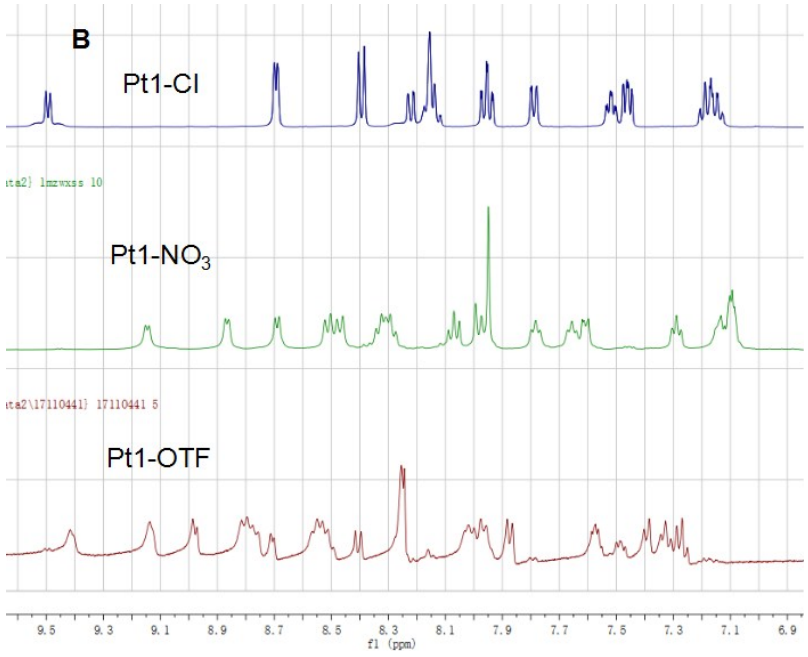
B
Pt1-Cl
Pt1-NO3
Pt1-OTF
9.5 9.3 9.1 8.9 8.7 8.5 8.3 8.1 7.9 7.7 7.5 7.3 7.1 6.9
f1 (ppm)

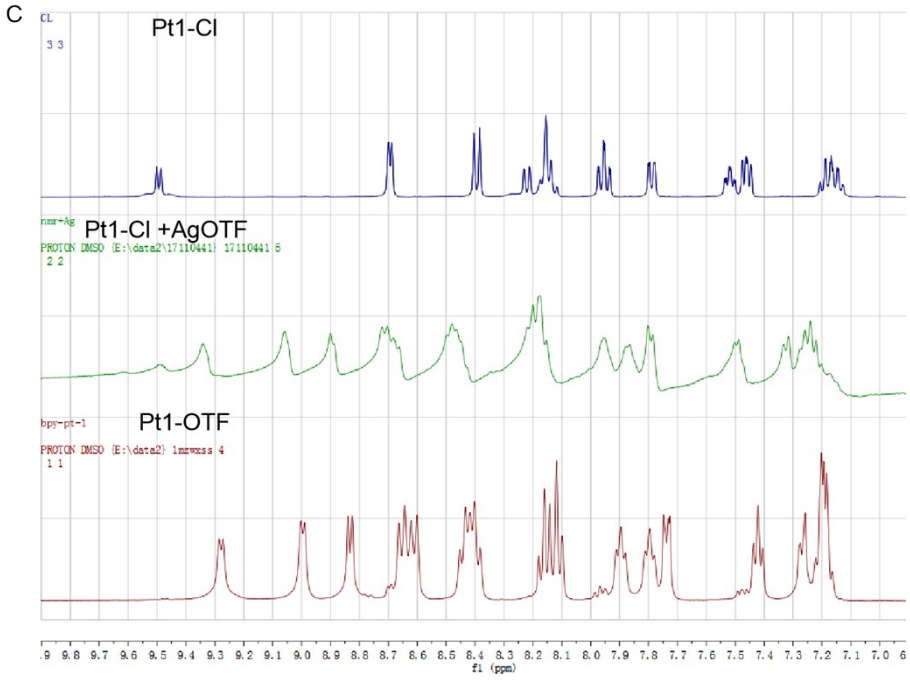

Fig. S4 The ^{1}H NMR stacking spectra (400 MHz, d_6-DMSO) of three Pt compounds at (A) 4.5 mM and (B) 0.4 mM, respectively; (C) The ^{1}H NMR spectra of **Pt1**-Cl (4.5 mM) in the presence of $AgCF_3SO_3$ (3-fold) in d_6-DMSO, indicating that the cationic part of **Pt1**-Cl is the same as **Pt1**-OTF.

(1)

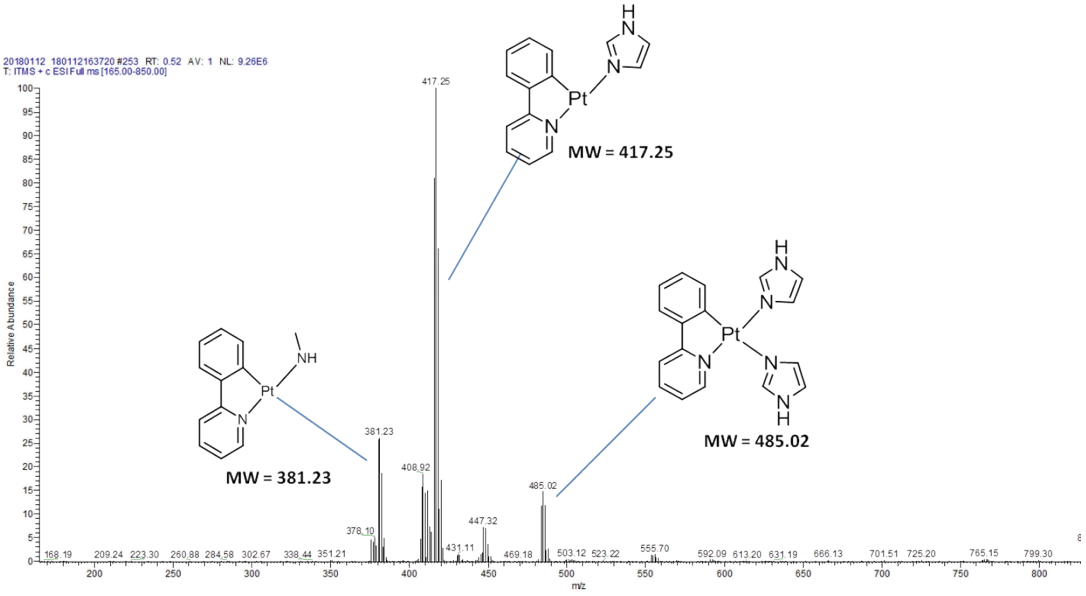

(2)

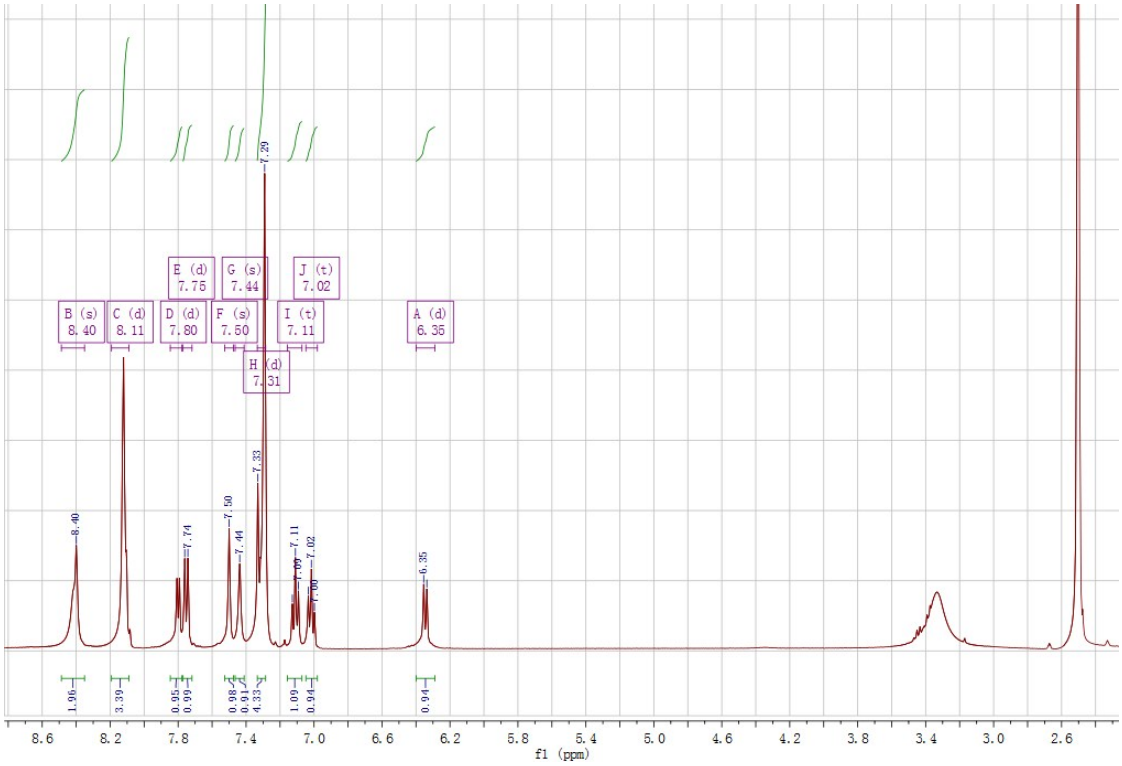

Fig. S5 (1) ESI-MS spectrum of **Pt2**; 485.02, $[M\text{-}CF_3SO_3^-]^+$; 417.25, $[M\text{-imazo-}CF_3SO_3^-]^+$ (2) ^1H NMR spectrum of complex **Pt2** (d_6-DMSO)

(1)

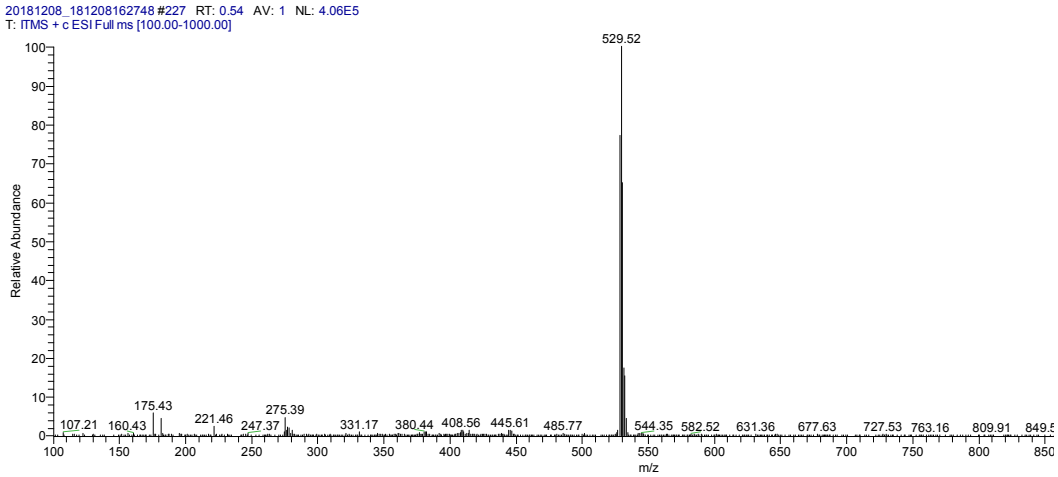

(2)

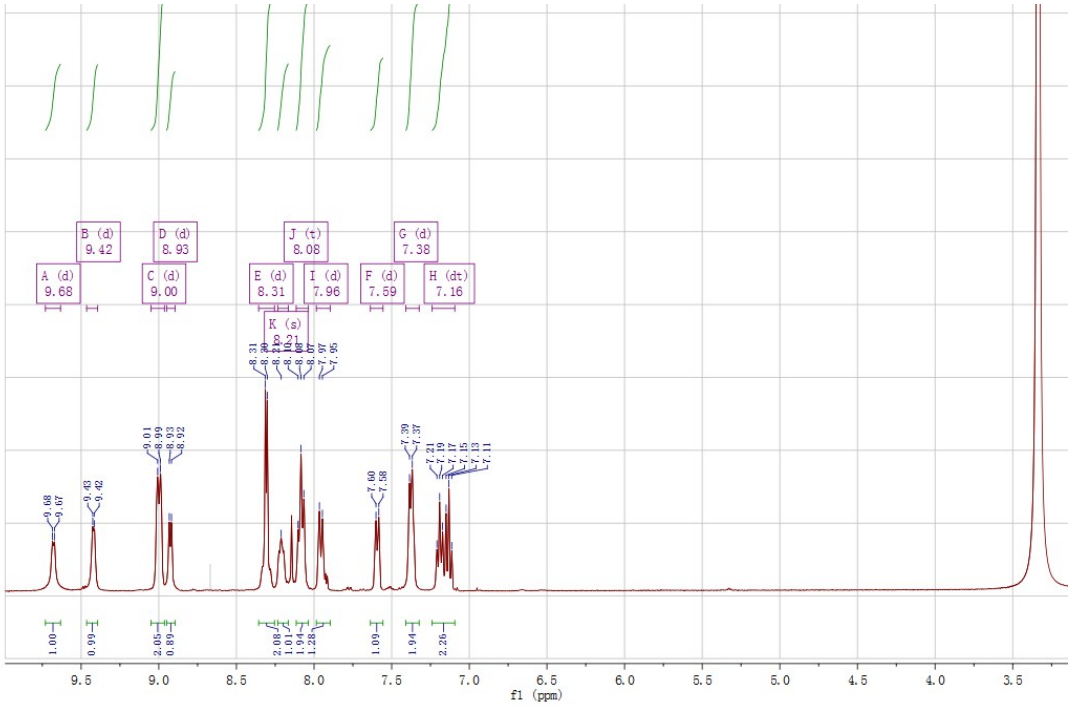

Fig. S6 (1) Positive ESI-MS spectrum of **Pt1a**; 529.52, $[M\text{-}CF_3SO_3^-]^+$; (2) ^1H NMR spectrum of complex **Pt1a** (d_6-DMSO)

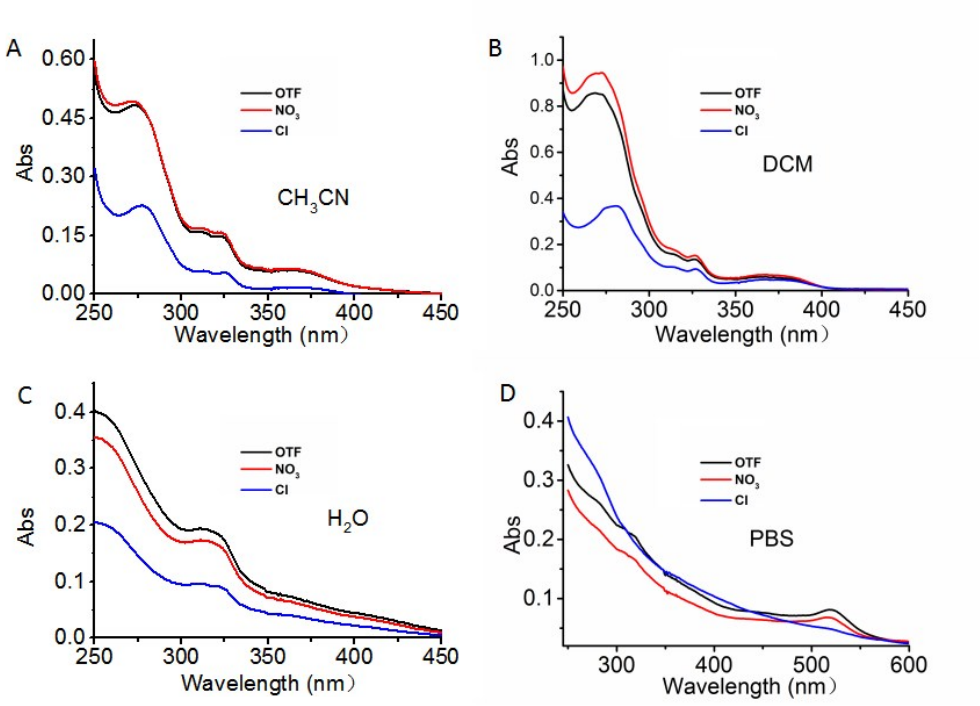

Fig. S7 UV-Vis spectra of complexes **Pt1**-(OTF, NO_3, Cl) (20 μM) in CH_3CN, DCM, H_2O and PBS.

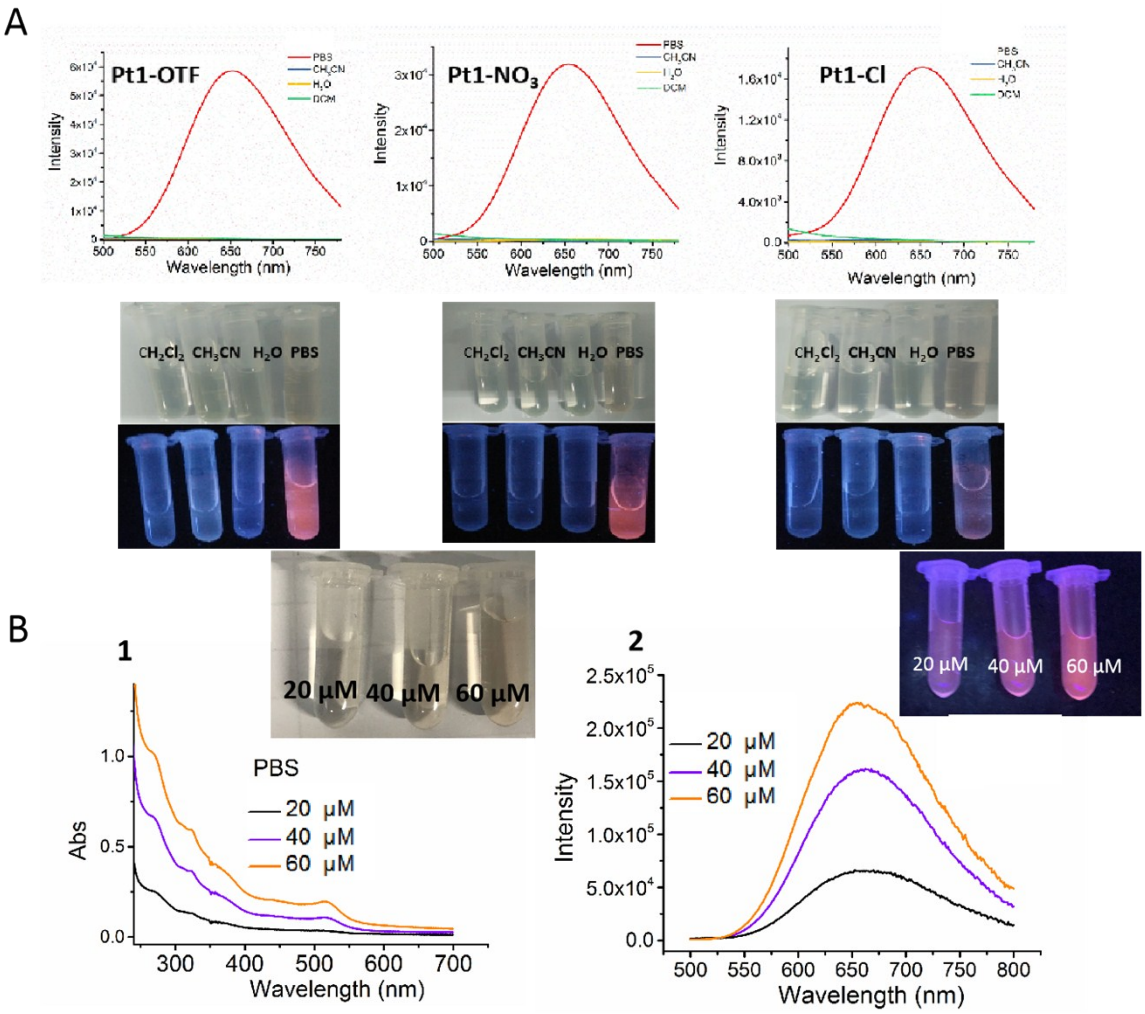

Fig. S8 A Luminescence spectra of complexes **Pt1**-(OTF, NO_3, Cl)(20 μM) in DCM, H_2O, CH_3CN and PBS (Photographs of **Pt1**-OTF, NO_3, Cl in corresponding solvent under sunlight (top) and UV lamp (bottom) **B** (1)UV-Vis spectra and (2) Luminescence spectra of complex **Pt1**-Cl in PBS of indicated concentration;

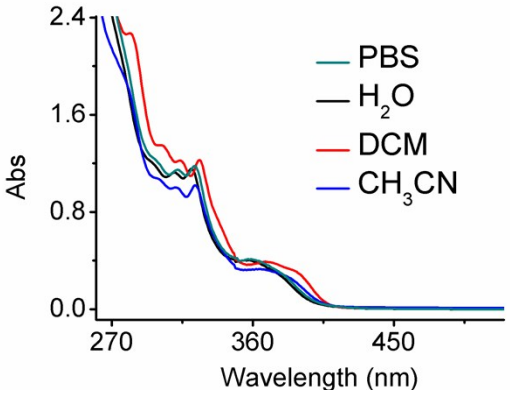

Fig. S9 UV-Vis spectra of complexes **Pt2**-OTF (30 μM) in CH_3CN, DCM, H_2O and PBS.

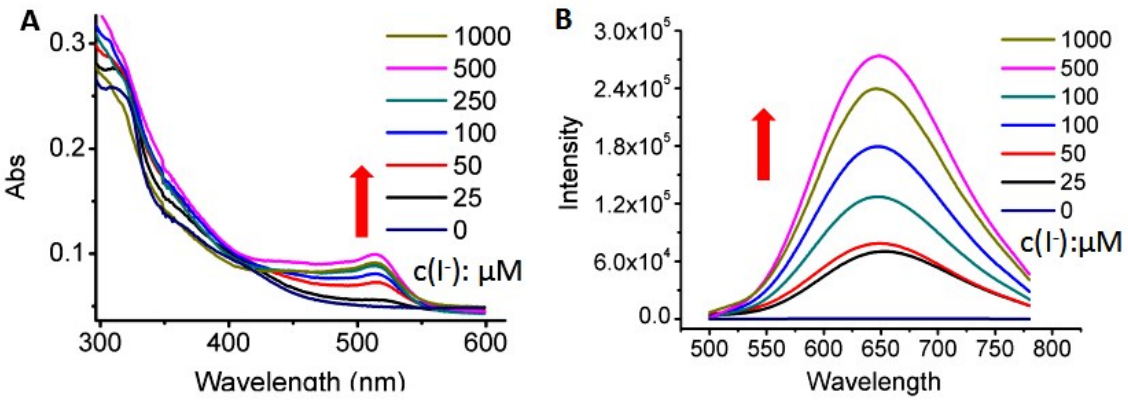

Fig. S10 (A)UV-Vis and (B) Emission titration spectra of **Pt1**-OTF (60 μM) recorded in H_2O with increasing concentrations of I^-.

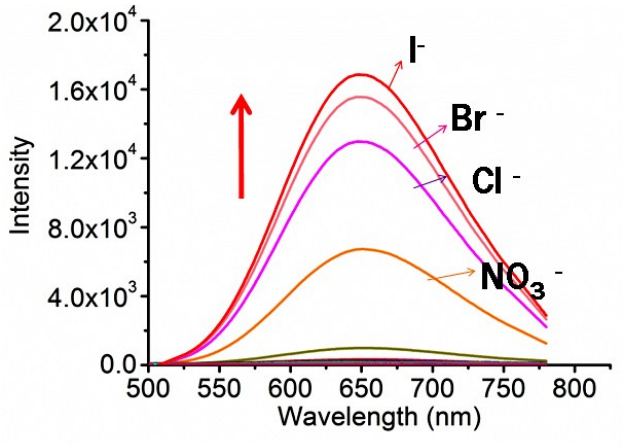

Fig. S11 Phosphorescence spectra of **Pt1**-OTF (50 uM) in aqueous media in the presence of tested anion (I^-, Br^-, Cl^-, F^-, HPO_4^-, BO_3^{3-}, HCO_3^{2-}, $Cr_2O_7^{2-}$, CO_3^{2-}, SO_4^{2-}, PO_4^{2-}, CH_3COO^-, NO_2^-, NO_3^-).;

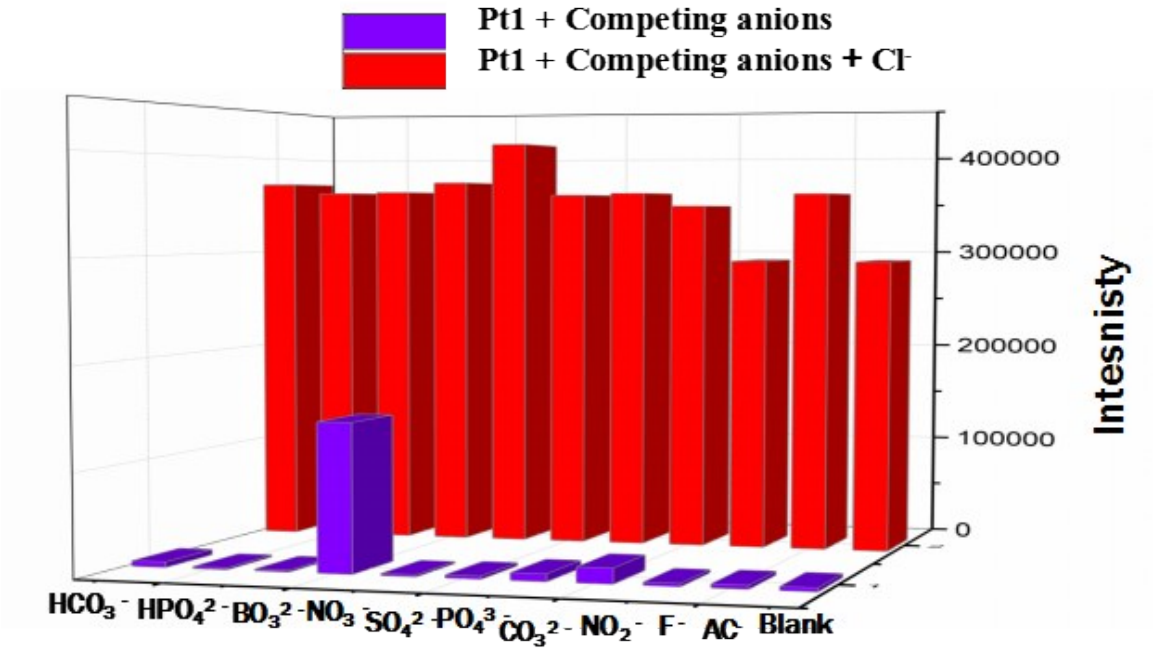

Fig. S12 Emission intensity of **Pt1**-OTF (20 μM) at 665 nm in the presence of indicated anions (80 equivalents) with/ without Cl^- (80 equivalents) in aqueous media. λex = 405 nm.

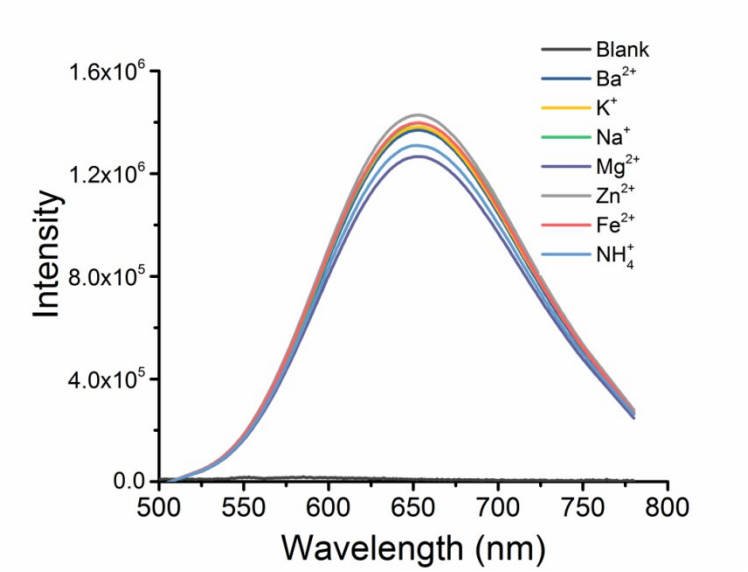

Fig. S13 Phosphorescence spectra of **Pt1**-OTF (20 μM) in the presence of various chlorides (150-fold equiv) in H_2O, the cations of which are Ba^{2+}, K^+, Na^+,Mg^{2+}, Zn^{2+},Fe^{2+},NH_4^+, respectively.

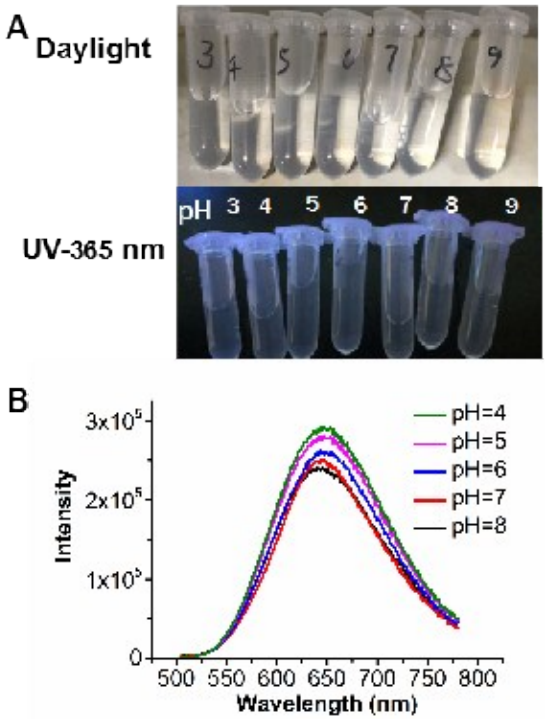

Fig. S14 (A)Photos of **Pt1**-OTF in Na_2HCO_3/Citric acid buffer system with different pH values 3.0-9.0 (as indicated) taken under the Daylight and 365 nm UV lamp;(B) Emission spectra of **Pt1**-OTF (20 μM) in the presence of Cl^- anions(100 equiv) in different pH (as indicated) aqueous media;

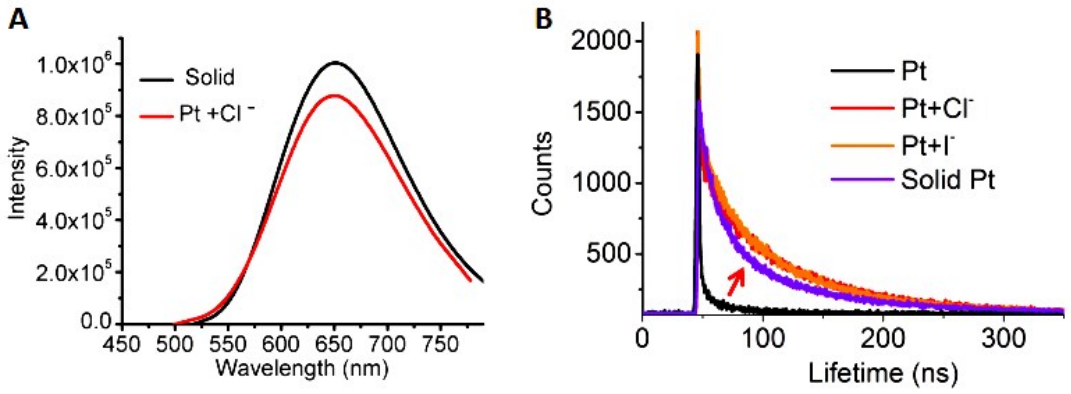

Fig. S15 (A) Emission spectra of **Pt1**-OTF in presence of Cl^- in aqueous media and solid state at room condition;.(B)Phosphorescence lifetimes decays of **Pt1** in absence and presence of Cl^- and I^- (80-fold equiv) in aqueous media and **Pt1** in the solid state.

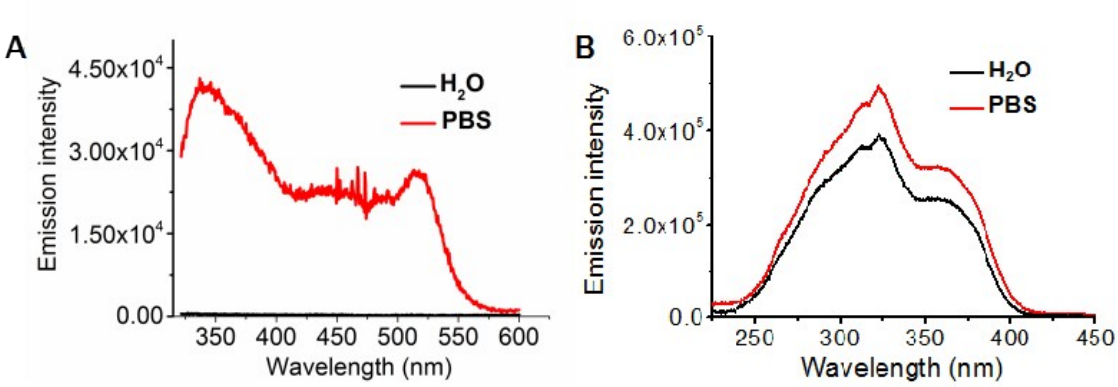

Fig. S16 Excitation spectra of (A) **Pt1**-OTF and (B) **Pt 2** (60 μM) in PBS and H_2O.

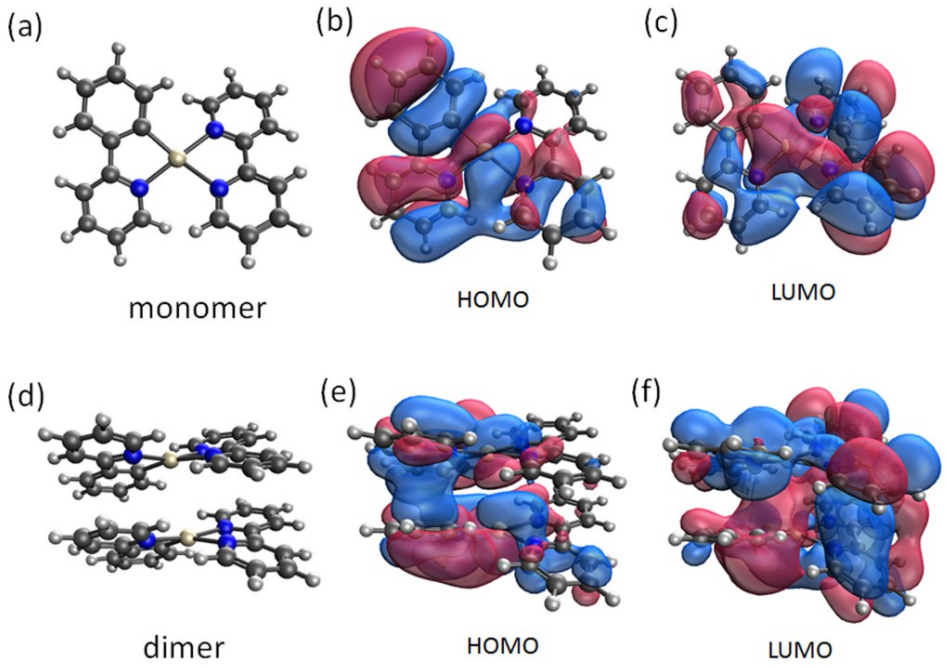

Fig. S17 DFT optimized structures of monomer and dimer of **Pt1** complex.

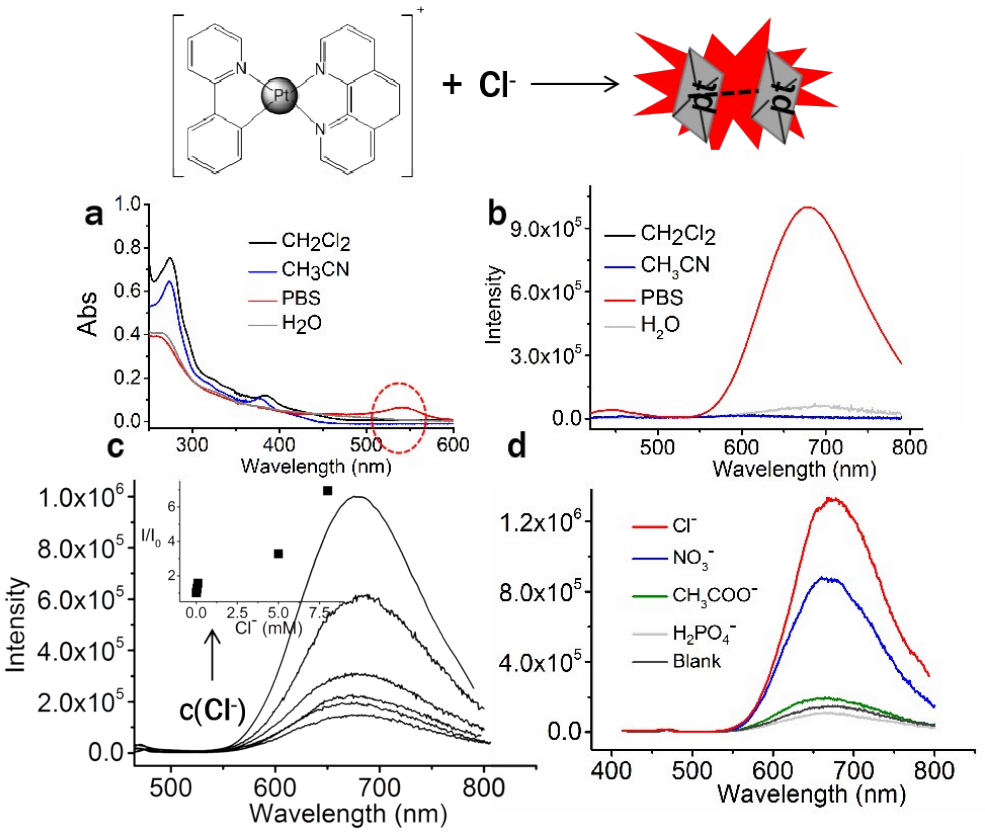

Fig. S18 Turn-on red phosphoresence of planar **Pt1a** complex induced by Cl^- anion in aqueous media: (a) UV-Vis and (b) Emission spectra of **Pt1a** (10 μM) in indicated solvent ; (c) Emission titration spectra of **Pt1**-OTF (60μM) recorded in H_2O with increasing concentrations of Cl^- as indicated; (d) Emission spectra of **Pt1a** (10 μM) in aqueous media in the presence of tested anion: Cl^-, NO_3^-, CH_3COO^-, $H_2PO_4^-$(4mM).

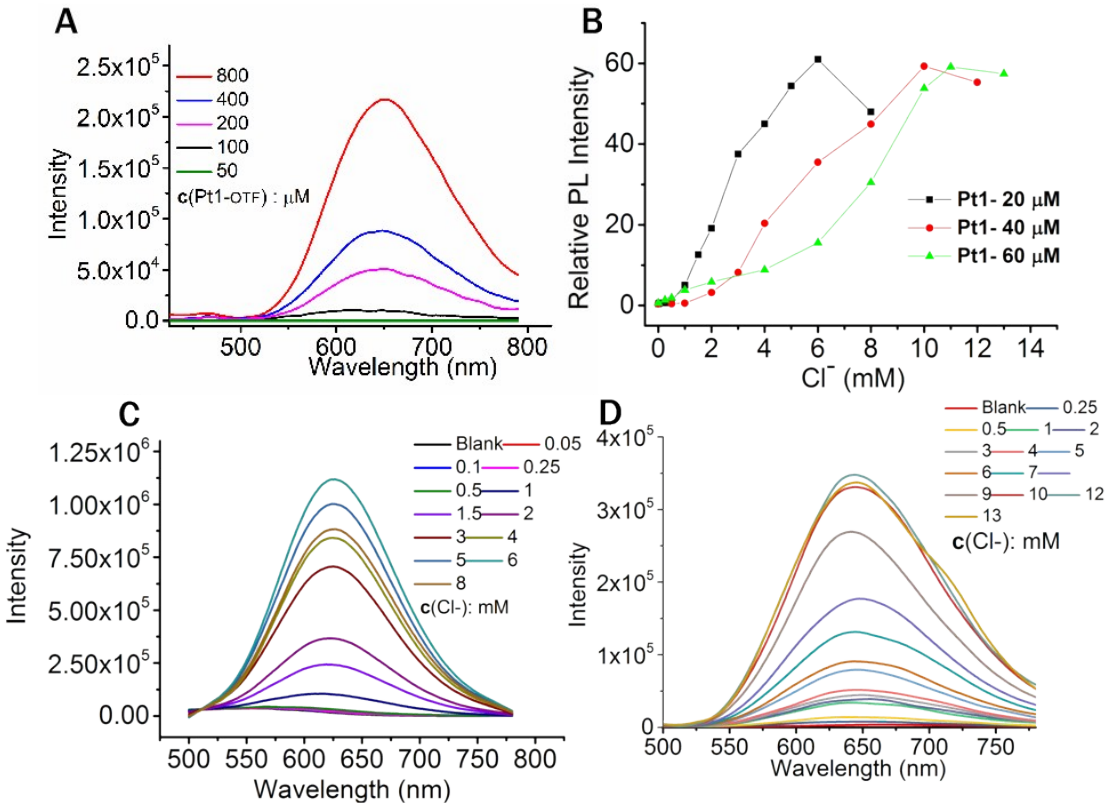

Fig. S19 (A) Emission spectra of **Pt1**-OTF with increasing concentration as indicated recorded in aqueous media.(B) Responsive range of enhanced "Turn-on"emission intensity of **Pt1**-OTF with different concentrations as indicated induced by Cl^- anion;(C) Emission titration spectra of **Pt1**-OTF (20 μM) and (D)(60 μM) recorded in H_2O with increasing concentrations of Cl^- as indicated; (The datas of 40 μM are shown in **Fig.2**)

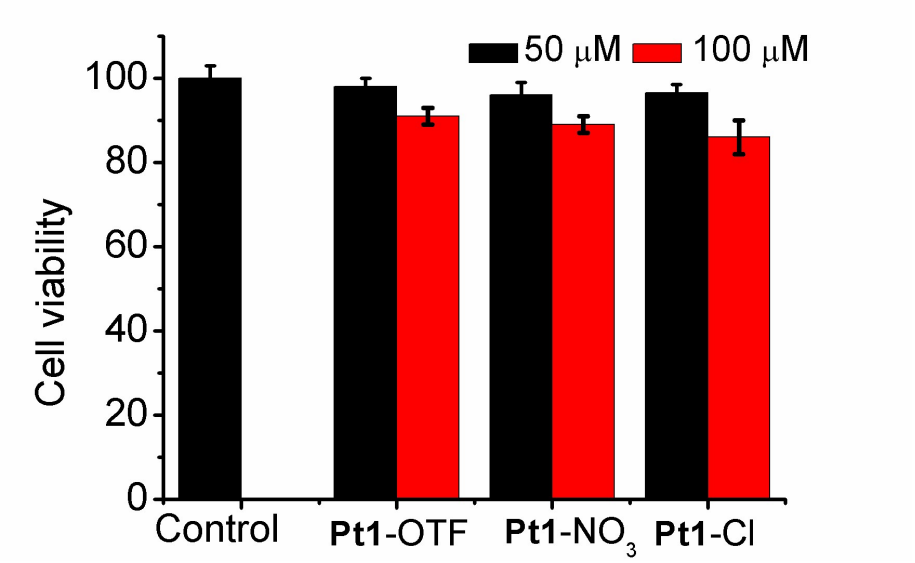

Fig. S20 Cell viability of MCF-7 treated with complexes of **Pt1**-(OTF, NO_3, Cl) (50 μM, 100 μM) for 48 h.

Table S1 Crystallographic data of **Pt1**-Cl

Empirical formula	C21H16N3PtCl
Formula weight	540.9
Temperature/K	100(2)
Crystal system	orthorhombic
Space group	I222
a/Å	3.68080(10)
b/Å	15.8713(6)
c/Å	18.2288(6)
α /°	90
β /°	90
γ /°	90
Volume/Å3	1064.91(6)
Z	2
ρ calcg/cm3	1.687
μ /mm-1	13.533
F(000)	516.0

Crystal size/mm3	0.018 ×0.013 × 0.011
Radiation	CuKα (λ = 1.54178)
2Θ range for data collection/°	7.386 to 152.428
Index ranges	-4 ≤ h ≤ 4, -19 ≤ k ≤ 15, -22 ≤ l ≤ 22
Reflections collected	2318
Independent reflections	1044 [R_{int} = 0.0694, R_{sigma} = 0.0439]
Data/restraints/parameters	1044/56/96
Goodness-of-fit on F2	1.164
Final R indexes [I>=2σ (I)]	R1 = 0.0634, wR2 = 0.1880
Final R indexes [all data]	R1 = 0.0636, wR2 = 0.1882
Largest diff. peak/hole / e Å-3	2.83/-1.80
Flack parameter	0.45(12)

Table S2 Selected bond lengths (Å) and bond angles (deg) of **Pt1-**Cl

Pt(1)-N(1)	2.043(17)	N(1)-Pt(1)-N(1^1)	79.4(9)
Pt(1)-(N1^1)	2.043(17)	N(1)-Pt(1)-N(1^2)	102.4(9)
Pt(1)-(N1^2)	2.043(17)	N(1)-Pt(1)-N(1^3)	165.6(12)
Pt(1)-(N1^3)	2.043(17)	N(1^2)-Pt(1)-N(1^3)	79.4(9)

Table S3 Crystallographic data of **Pt2**-OTF

Empirical formula	$C_{18}H_{16}F_3N_5O_3PtS$
Formula weight	634.51
Temperature/K	120.0
Crystal system	monoclinic
Space group	C2/c
a/Å	17.1449(7)
b/Å	9.2946(3)
c/Å	26.3630(10)
α/°	90
β/°	92.9640(10)
γ/°	90
Volume/Å3	4195.5(3)
Z	8
ρcalcg/cm3	2.009
μ/mm-1	6.845
F(000)	2432.0
Crystal size/mm3	0.149 × 0.086 × 0.057
Radiation	MoKα (λ = 0.71073)
2Θ range for data collection/°	4.758 to 56.698
Index ranges	$-22 \leq h \leq 22$, $-12 \leq k \leq 9$, $-35 \leq l \leq 35$
Reflections collected	18878
Independent reflections	5181 [Rint = 0.0478, Rsigma = 0.0448]
Data/restraints/parameters	5181/24/280
Goodness-of-fit on F2	1.043
Final R indexes [I>=2σ (I)]	R1 = 0.0271, wR2 = 0.0628
Final R indexes [all data]	R1 = 0.0348, wR2 = 0.0651
Largest diff. peak/hole / e Å-3	1.28/-1.24

Table S4 Selected bond lengths (Å) and bond angles (deg) of **Pt2**-OTF

bond lengths (Å)		bond angles (deg)	
Pt(1)-C(1)	1.994(4)	C(1)-Pt(1)-N(2)	81.06(14)
Pt(1)-N2	2.014(3)	C(1)-Pt(1)-N(3)	176.28(13)
Pt(1)-N3	2.068(3)	N(2)-Pt(1)-N(5)	176.72(13)
Pt(1)-N5	2.049(3)	C(1)-Pt(1)-N(5)	95.77(14)

Table S5. The DFT calculations of transition from the ground state (S0) to the excited state S1 of monomer and dimer of **Pt1** complex.

	Energy/eV	**λ/nm**	**Oscillator strength**	**Nature of transition**	**Orbital contribution**
Pt1 monomer	2.76	448.75	0.0333	MLCT	HOMO-LUMO
Pt1dimer	2.51	494.77	0.0045	MMLCT	HOMO-1-LUMO+1 (3.12%) HOMO-LUMO (73.85%) HMO-LUMO+1(23.02)

Reference

1. P.I.Kvam, J.Songstad, Acta.*Chem.Scand*., 1995, **49**, 313-324.

2. D. M. Jenkins, J. F. Senn, S. Bernhard, *Dalton. Trans.*, 2012, **41**, 8077-8085

3. G. M.Sheldrick, *Acta. Crystallogr. Sect. A,* 2008, **64**, 112-122.

4. 4. G. A. Crosby and J. N. Demas, *The J. Physi. Chem*.,1971,**75**, 991-1024.

5. D. Pucci, A. Bellusci, A. Crispini, M. Ghedini, N. Godbert, E. I. Szerb, A. M. Talarico, *J. Mater.,Chem.*, 2009, **19**, 7643-7649.

6. P. Hohenberg , W. Kohn, *Phys. Rev.*,1964, **136**, B864 -B871.

7. W.Kohn, L.J.Sham, *Phys. Rev.*, 1965, **140**, A1133−A1138.

8. M. J. Frisch, G. W. Trucks, H. B. Schlegel, G. E. Scuseria, M. A. Robb, J. R. Cheeseman, G. Scalmani, V. Barone, B. Mennucci, G. A. Petersson, H. Nakatsuji, M. Caricato, X. Li, H. P.

Hratchian, A. F. Izmaylov, J. Bloino, G. Zheng, J. L. Sonnenberg, M. Hada, M. Ehara, K. Toyota, R. Fukuda, J. Hasegawa, M. Ishida, T. Nakajima, Y. Honda, O. Kitao, H. Nakai, T. Vreven, J. A. Montgomery, Jr., J. E. Peralta, F. Ogliaro, M. Bearpark, J. J. Heyd, E. Brothers, K. N. Kudin, V. N. Staroverov, R. Kobayashi, J. Normand, K. Raghavachari, A. Rendell, J. C. Burant, S. S. Iyengar, J. Tomasi, M. Cossi, N. Rega, J. M. M. Millam, M. Klene, J. E. K. Knox, J. B. C. Cross, V. Bakken, C. Adamo, J. Jaramillo, R. Gomperts, R. E. Stratmann, O. Yazyev, A. J. Austin, R. Cammi, C. Pomelli, J. W. Ochterski, R. L. Martin, K. Morokuma, V. G. Zakrzewski, G. A. Voth, P. Salvador, J. J. Dannenberg, S. Dapprich, A. D. Daniels, O. Farkas, J. B. Foresman, J. V. Ortiz, J. Cioslowski and D. J. Fox, Gaussian 09, Revision D.01, Gaussian, Inc.:Pittsburgh, PA, 2009.

9. Y. Zhao, D. G.Truhlar, *Theor. Chem. Acc.,* 2008, **120**, 215−241.
10. L. Zhang, Y. Zhang, H. Tao, X. Sun, Z. Guo, L. Zhu, *J. Mol. Struc.TheoChem.*, 2002, **617**, 87-97.
11. R. E. Stratmann, G. E. Scuseria, M. J. Frisch, *J. Chem. Phys.*, 1998, **109**, 8218–82244